

# Statistical Process Monitoring of Nonlinear Profiles Using Wavelets

Eric Chicken\*

Department of Statistics  
Florida State University  
Tallahassee, FL 32306

Joseph J. Pignatiello, Jr.  
James R. Simpson

Department of Industrial and Manufacturing Engineering  
Florida State University  
Tallahassee, FL 32310-6046

## Abstract

Many modern industrial processes are capable of generating rich and complex data records that do not readily permit the use of traditional statistical process control techniques. For example, a “single observation” from a process might consist of  $n$  pairs of  $(x, y)$  data that can be described as  $y = f(x)$  when the process is in-control. Such data structures or relationships between  $y$  and  $x$  have been called profiles. A few examples of such profiles include calibration curves in chemical processing, oxide thickness across wafer surfaces in semiconductor manufacturing and radar signals of military targets. In this paper, a semiparametric wavelet method is proposed for monitoring for changes in sequences of nonlinear profiles. No assumptions are made on the nature of form or the changes between the profiles other than finite square-integrability. Based on a likelihood ratio test involving a changepoint model, the method uses the spatial adaptivity properties of wavelets to accurately detect profile changes taking nearly limitless functional forms. Performance of the method is assessed

---

*Key words and phrases.* Average run length, change point, control charts, likelihood ratio, nonlinear profiles, profile monitoring, profiling, semiparametric, statistical process control, thresholding, wavelets.

\*Corresponding author: email [chicken@stat.fsu.edu](mailto:chicken@stat.fsu.edu)

with Monte Carlo simulation. The results presented indicate the method can quickly detect a wide variety of changes from a given, in-control profile.

# 1 Introduction

Traditional statistical process control (SPC) charts have been widely used to monitor processes for changes in means, standard deviations, fraction nonconforming and Poisson rates. Multivariate control charts are also available to monitor for changes in mean vectors and covariance matrices. These control charts have been successfully used for monitoring processes for many years.

In many modern industrial processes, massive amounts of data are often readily available and in complex data structures that may not be readily or best addressed by the traditional control charts. For example, a “single observation” on an in-control process might consist of a functional realization of  $n$  pairs of  $(x, y)$  data that can be described by  $y = f^0(x) + \epsilon$  where  $f^0$  is a known function and  $\epsilon$  is random noise with mean zero and standard deviation  $\sigma$ . Thus, an observation on the process is a realization of a dependent variable  $y$  at  $n$  values of  $x$ .

In manufacturing, the quality of some products might be determined by a relationship between two variables. For example, an electronic circuit’s output signal  $y$  must follow a prescribed functional pattern when the input voltage  $x$  varies over a specified range. That is,  $y = f^0(x) + \epsilon$ , where  $f^0$  is the prescribed functional relationship between the input voltage and the circuit’s output signal. To check the calibration of a scale or thermometer, the relationship between a known load or temperature and the scale’s or thermometer’s output reading must be true for all values of load or temperature within a given standard range.

Another instance of functional forms as a response variable is in the analysis of radar signals. Here,  $f^0$  is a known radar signature, either of a specified object such as an aircraft, or of a static surveilled field. In national security and civilian safety applications, it is critical to identify changes in such functional responses.

Such data structures or relationships between  $y$  and  $x$  have been called profiles. A few examples of such profiles include calibration curves in chemical processing (Stover and Brill (1998)), oxide thickness across wafer surfaces in semiconductor manufacturing (Gardner et al. (1997)) and the stamping force as a function of crank arm angle in a steel stamping operation (Jin and Shi (1999)). In instances such as these, it is desirable to determine when a change in the profile has occurred, as this indicates that the process is out-of-control.

Various control chart methods have been applied to the profile monitoring situation. Woodall et al. (2004) provide an excellent overview of the SPC literature involving profiles. A number of studies have investigated linear profiles where the functions are simple straight lines. Many of these approaches focus on monitoring for changes in the intercept, slope and error standard deviation. For example, Mahmoud et al. (2007) used a changepoint formulation to monitor for changes in regression coefficients. Stover and Brill (1998) used a Hotelling  $T^2$  chart to monitor for changes in the parameters of a simple linear profile. Like other Shewhart control charts, the Hotelling  $T^2$  chart (Montgomery (2005)) only uses information from the current sample to assess whether the process is in state of control. Control charts that accumulate or incorporate information from previous samples, such as CUSUM and EWMA charts, are known to be more sensitive to moderate to small changes in process parameters. Kang and Albin (2000) showed that a univariate EWMA chart that monitors the average residual between observed and target linear profiles is more sensitive than a Hotelling's  $T^2$  chart that monitors slope and intercept parameters. They also used an  $R$  chart in conjunction with the EWMA chart to counteract the possibility that extreme residuals of opposite sign would go undetected. Kim et al. (2003) further improved the detection of parameter changes by using independent EWMA charts applied separately to each parameter. To remove covariance between the slope and intercept estimates, they first transformed the independent variable so that its average value was zero. One problem with monitoring the parameters of a linear profile is that a process could change such that the resulting profile is no longer linear yet a straight line fit could yield the same parameter

estimates. Thus, the lack of linearity could go unnoticed.

While it appears that EWMA charts can perform well when monitoring for changes in linear profile parameters, there are many instances when the form of the profile is nonlinear or otherwise too complicated to express as a parametric function. For example, Williams et al. (2007) consider multivariate nonlinear parametric forms for profiles. However, modeling profiles parametrically has drawbacks. As with linear modeling, it is possible for a profile to change, yet the parameter estimates remain the same. Additionally, it may be difficult to specify a correct parametric model to fit a particular profile.

In this paper, a method is proposed for detecting changes in a sequence of profiles that is not dependent on strong assumptions on the form of the profiles. Such a method will by necessity include nonparametric tools. For example, Gardner et al. (1997) used a smoothing spline to model semiconductor wafer thickness at selected locations along the wafer surface. Williams et al. (2007), in addition to using parametric models as mentioned above, also considered nonparametric forms for estimating profiles. They too examine the utility of spline smoothing methods for profile monitoring.

The method of using splines belongs to a large class of nonparametric estimators which smooth the data. Such smoothing estimators have fewer restrictions than parametric methods, but their smoothing property may be undesirable. If the profiles contain explicitly unsmooth features (jumps, or points of non-differentiability, for example) smoothing estimators will not model such features well. In Williams et al. (2007), the use of the smoothing spline is not unreasonable given their particular, smooth application data. Actually, the data examined in that paper lends itself so well to parameterization that the nonlinear parametric method appears to be preferable. The methods they examine, both parametric and nonparametric, give quite different results when monitoring for differences among the profiles. In general, when a profile can be accurately modeled via parametric means (for example, as a line), then methods taking advantage of such assumptions should be considered.

The assumption of smoothness, whether for parametric or nonparametric analysis, is

not always valid. There are instances when the change from one profile to the next is neither smooth or parameterizable. A method for more general differences is needed.

In this paper, the focus is on detecting a change from a known or estimated in-control profile, to a new, out-of-control profile. The proposed approach involves examining the differences of each new profile from the in-control profile. Under previous linear profiling models, these differences were also restricted to be straight lines. That is, the changed profiles are assumed to be other straight lines with different slopes and/or intercepts. However, our proposed approach allows much more general differences between profiles by only requiring that the differences be functions in the class of finite  $L^2$  functions. That is, the differences between the in-control profiles  $f^0$  and the out-of-control profiles  $f^1$  are merely required to be such that

$$\|f^1 - f^0\|_{L^2}^2 = \int_a^b (f^1(x) - f^0(x))^2 dx < \infty, \quad (1)$$

where  $[a, b]$  is the common support of the profiles. This constitutes a very large class of functions for profiles and their differences, including very unsmooth function differences that nonparametric smoothers such as those in Williams et al. (2007) and Gardner et al. (1997) would not handle well. Other measures of the differences exist. Williams et al. (2007) examine several in addition to  $L^2$ .

Since the functions, and hence their differences, may come from a large class of functions, the use of wavelets is proposed for approximating or estimating the functions and the differences between them. The wavelet property of spatial adaptivity can be exploited to accurately represent functions without restricting or knowing much about their form ahead of time. Wavelets also bypass the problem inherent in nonparametric estimators such as spline smoothing: they model quite well features such as jumps or non-differentiable points.

Wavelets are very efficient at function approximation. They excel at spatial adaptivity, optimality in terms of error rates, and low computational cost. Typically, wavelet analysis is performed through the use of thresholding of wavelet coefficients, such as the VisuShrink method of Donoho and Johnstone (1994) or block methods of Cai (1999), Chicken (2003,

2005) and Chicken and Cai (2005). In these instances, a noisy function is transformed into wavelet coefficients by the discrete wavelet transform (DWT) of Mallat (1989). These coefficients are then modified by comparison with a specified thresholding rule, and the underlying function is estimated by applying the inverse DWT to these modified coefficients. The result is a “denoised” function, that is, an estimate of the true underlying function with noise removed.

Examples of the use of wavelets for profiles may be found in Jeong et al. (2006), Jin and Shi (2001) and Fan (1996). They used wavelets to detect changes from one profile to the next by observing the magnitudes of the coefficients from a profile’s DWT. Their methods assumed Gaussian noise, but used this assumption only to test the sum of the squared profile wavelet coefficients.

In this paper, a different wavelet analysis approach is employed for profile monitoring. One of these differences is the introduction of changepoint analysis into the estimation. Changepoint methods have been considered previously in profile methods, though not in conjunction with the use of wavelets. Mahmoud et al. (2007) and Zou et al. (2006) considered linear profiles, while Ding et al. (2006) examined nonlinear profiles. Ding et al. (2006) used independent component analysis (ICA) to reduce the profiles to a set of components which were likely to model differences among profiles. After this data- and dimension-reduction step, changepoint methods were applied to the components to detect changes in profiles. They considered only horizontal shifts as the difference between profiles. The wavelet estimator proposed in this paper does not restrict itself to such differences between profiles, but allows for much more extensive changes.

For the proposed new wavelet method, a changepoint formulation is used to develop a likelihood ratio test statistic under the assumption of Gaussian errors and utilizing the orthogonality property of the DWT. Use is made of the wavelet’s optimal estimation properties (Donoho and Johnstone (1994)) to determine the values of parameters within this statistic. By incorporating these wavelet properties and the information prior to the changepoint into

the estimates, marked improvements in performance compared to Jeong et al. (2006), Jin and Shi (2001) and Fan (1996) can be realized.

In addition to the introduction of changepoint estimation and prior information, the proposed method differs from previous methods in its use of wavelets. The current wavelet methods cited above monitor the wavelet coefficients, perhaps modifying them through thresholding. Since differencing is applied to the in-control and out-of-control profiles, this is equivalent to observing sequences of normal (or perhaps truncated normal, if wavelet thresholding is used) random variables.

The novel approach taken here is to use wavelet thresholding to accurately estimate a parameter integral to the evaluation of the likelihood ratio. The optimal properties of wavelets provide accurate estimation of this parameter via nonlinear thresholding, leading to an efficient method of detecting profile changes. The proposed estimator thus uses wavelets for two purposes: a nonparametric estimate of the size of the difference between two profiles; and an efficient estimate of an essential likelihood parameter.

Thresholding of wavelets can also be thought of as an analog to the use of ICA in Ding et al. (2006). First, both are data reduction methods. Second, the profile projections created by ICA may be used to isolate differences between profiles that are not due to Gaussian noise. Similarly, thresholding the wavelet projections of a profile gives that portion of a profile that has had the differences due to noise removed.

The proposed profile monitoring control chart statistic is based on a likelihood ratio test for a changepoint model. The likelihood is determined by making distributional assumptions on the errors in the profiles, and requires estimation of a specific parameter. In this sense, the method is parametric. However, the likelihood test uses wavelet estimation of unknown profiles and hence incorporates nonlinear, nonparametric methods. Therefore, the proposed approach can be considered to be nonlinear and semiparametric.

In this paper, processes to be monitored generate data where each sample consists of  $n$  pairs of points  $(x_i, y_i)$ ,  $i = 1, 2, \dots, n$ . When the process is in-control, the relationship

between  $y$  and  $x$  is assumed to be known with  $y = f^0(x) + \epsilon$ , where  $\epsilon$  is a random error with mean zero and standard deviation  $\sigma$ . Either  $f^0$  is known, a strong assumption, or it is estimated using several observed noisy profiles which are assumed to be in-control. While Ding et al. (2006) examines changes in variability from one profile to the next, it is assumed here that the variances are constant within and across profiles. Changing this assumption is a topic for future study.

The remainder of this paper is organized as follows. Section 2 presents a brief background on wavelets. The profile monitoring problem is formulated in Section 3. In Section 4, a likelihood ratio test for the profile changepoint problem is developed along with a control chart for monitoring profiles. The performance of the proposed control chart is then evaluated and compared with results from those of competitors.

## 2 Wavelets and Multiresolution Analysis

Wavelets are an orthogonal series representation of functions in  $L_2(R)$ , the space of square-integrable functions. Vidakovic (1999) and Ogden (1997) offer good introductions to wavelet methods and their properties. It is common to let  $\phi$  and  $\psi$  represent the father and mother wavelet functions, respectively. There are large families of choices for these two functions available for use, see for example Daubechies (1992). Here,  $\phi$  and  $\psi$  are chosen to be compactly supported and to generate an orthonormal basis. Let  $\phi_{jk}(x) = 2^{j/2}\phi(2^jx - k)$  and  $\psi_{jk}(x) = 2^{j/2}\psi(2^jx - k)$  be the translations and dilations of  $\phi$  and  $\psi$ , respectively, where  $j$  and  $k$  are integers. Then for any fixed integer  $j_0$ ,  $\{\phi_{j_0k}, \psi_{j_0k} | j \geq j_0, k \text{ an integer}\}$  is an orthonormal basis for  $L_2(R)$ . Let  $\xi_{jk} = \langle f, \phi_{jk} \rangle$  and  $\theta_{jk} = \langle f, \psi_{jk} \rangle$  be the usual inner product of a function  $f \in L_2(R)$  with the wavelet basis functions. Then  $f$  can be expressed as an infinite series

$$f(x) = \sum_k \xi_{j_0k} \phi_{j_0k}(x) + \sum_{j=j_0}^{\infty} \sum_k \theta_{jk} \psi_{jk}(x).$$

In general,  $f$  need not be known but at least a discrete realization of it must be available. Therefore, the wavelet coefficients can be estimated using the DWT. If  $f$  is represented as a vector of dyadic length  $n = 2^J$  for some positive integer  $J$ , then the DWT will provide a total of  $n$  estimated coefficients  $\xi_{j_0k}$  and  $\theta_{jk}$  over the indices  $j = j_0, j_0 + 1, \dots, J - 1$  and for all appropriate  $k$ . The lowest level possible for  $j_0$  is 0, but higher values may be chosen.

Wavelets have the useful property that they can simultaneously analyze a function in both the x-axis and frequency domains. This is accomplished through the series representation for  $f$  mentioned above and can be viewed as several series: one series involving the father wavelet at level  $j_0$ , and one mother wavelet-based series for each  $j \geq j_0$ . The first series corresponds to the smooth, or coarse, structure of  $f$ . The other series correspond with increasingly detailed, higher-frequency parts of  $f$ . Changing the index (or resolution level)  $j$  allows one to zoom in or out onto the smooth or detailed structure of  $f$ . This is referred to as the multiresolution property of wavelets. This property enables wavelets to model functions of very irregular type, as well as smoother functions.

### 3 A Changepoint Model for Modeling Nonlinear Profiles with Wavelets

Suppose there are  $T$  samples or profiles  $(x_1, y_1^t), (x_2, y_2^t), \dots, (x_n, y_n^t)$  available, where  $t = 1, 2, \dots, T$ . The relationship between  $y$  and  $x$  is assumed to be of the form  $y = f(x)$ . Since the data are collected in an experimental fashion, what is observed is  $y_i^t = f^t(x_i) + \varepsilon_i^t$  for  $t = 1, 2, \dots, T$ ,  $i = 1, 2, \dots, n$ , with the  $x_i$  equispaced over the interval. The errors  $\varepsilon_i^t$  are assumed to be independent, identically distributed normal( $0, \sigma^2$ ) random variables.

Consider the case where there is a point  $t = \tau$  in the sequence of profiles after which the profiles change:  $f^1 = f^2 = \dots = f^\tau \neq f^{\tau+1} = f^{\tau+2} = \dots = f^T$ . In statistical profile monitoring, one is interested in detecting the change in the profiles as soon after the changepoint  $\tau$  as possible, as well as estimating  $\tau$  once the change has been detected.

Previous work on profile monitoring assumed that the functions  $f$  were linear or that the differences between profiles is linear or piecewise linear. Such restrictions can be significantly relaxed and generalized by considering the differences to be nearly arbitrary functions. Since these difference functions are general, wavelets can be used to estimate them.

The wavelet transformation is performed on the observed data  $\mathbf{y}^t = \{y_i^t\}$  for a fixed  $t$ . Each profile is assumed to be of length  $n$ , with  $n$  a dyadic integer,  $n = 2^J$ . The transformation is given by

$$\tilde{\boldsymbol{\theta}}^t = n^{-1/2} \mathbf{W} \mathbf{y}^t = n^{-1/2} \mathbf{W} (\mathbf{f}^t + \boldsymbol{\varepsilon}^t) = \boldsymbol{\theta}^t + n^{-1/2} \mathbf{W} \boldsymbol{\varepsilon}^t$$

where  $\mathbf{W}$  is the  $n \times n$  orthonormal wavelet transformation matrix (Mallat (1989)) and  $\boldsymbol{\theta}^t$  is the wavelet transformation of the true (unobserved) sampled function  $\mathbf{f}^t$ . Since  $\mathbf{W}$  is an orthogonal transformation,  $\tilde{\boldsymbol{\theta}}^t$  is normal with mean  $\boldsymbol{\theta}^t$  and variance  $\sigma^2/n \cdot \mathbf{I}_{n \times n}$ . Thus, there are multiple vectors  $\tilde{\boldsymbol{\theta}}^t$  of the form

$$\tilde{\boldsymbol{\theta}}^t = \{\tilde{\xi}_{0,1}^t, \tilde{\theta}_{0,1}^t, \tilde{\theta}_{1,1}^t, \tilde{\theta}_{1,2}^t, \tilde{\theta}_{2,1}^t, \tilde{\theta}_{2,2}^t, \tilde{\theta}_{2,3}^t, \tilde{\theta}_{2,4}^t, \tilde{\theta}_{3,1}^t, \dots, \tilde{\theta}_{J-2,2^{J-2}}^t, \tilde{\theta}_{J-1,1}^t, \dots, \tilde{\theta}_{J-1,2^{J-1}}^t\}$$

each of length  $n$ , one for each profile. Each vector is partitioned or organized as follows: the first component represents the coarsest, smoothest part of the function. The next component is the next coarsest part, the next two components are the next coarsest after that, etc. The last  $n/2 = 2^{J-1}$  components represent the finest details of the original data  $\mathbf{y}^t = \{y_i^t\}$ . The decomposition need not start at level 0, but can start at any integer  $j_0 < J$ . Since the two coarsest parts reside in the same resolution space, there is a notation difference ( $\theta$  vs  $\xi$ ). For simplicity, the vector of wavelet coefficients  $\tilde{\boldsymbol{\theta}}^t = \{\tilde{\theta}_i^t\}$  is relabeled with a single index  $i$  where  $i = 1, 2, \dots, n$ .

Below, with each newly observed sample profile,  $(x_i, y_i^t)$ ,  $i = 1, 2, \dots, n$ , the true  $\boldsymbol{\theta}^t$  is estimated with  $\tilde{\boldsymbol{\theta}}^t$  to determine if  $f^t$  has changed from the known in-control function  $f^0$ . This is done by comparing the  $\tilde{\boldsymbol{\theta}}^t$  wavelet vectors to the  $\boldsymbol{\theta}^0$  wavelet vector (or its estimate) via a likelihood ratio.

## 4 Development of a Control Chart for Monitoring Non-linear Profiles

A likelihood ratio test involving a changepoint model for the statistical monitoring of profiles is now considered. In the next section, the performance of this proposed approach is evaluated and compared with others.

### 4.1 Hypotheses Under the Changepoint Model

Let  $t = 1, 2, \dots, T$  be the indices for the profile sequence  $\mathbf{f}^t$ , where  $T$  represents the most recently observed profile. The null hypothesis under consideration is that the profiles are always in control:

$$H_0 : \|f^t - f^0\|_{L^2}^2 = \int_0^1 (f^t(x) - f^0(x))^2 dx = 0, \quad t = 1, 2, \dots, T$$

where for simplicity it is assumed that the common support of the profiles is  $[a, b]$  is  $[0, 1]$ . The  $L_2$  norm is a measure of the distance between two profiles. The alternative hypothesis is that the profiles are different from  $f^0$  in terms of the norm of their difference after some unknown time  $\tau$ . That is,

$$H_a : \|f^t - f^0\|_{L^2}^2 > 0, \quad t = \tau + 1, \tau + 2, \dots, T.$$

Since the integrated difference between the two profiles is assumed to be finite, wavelets will be used to accurately estimate this difference (Vidakovic (1999)). Functional forms for the  $f^t$  are not necessarily known or required beyond this simple assumption. The norm of the difference in the functions in  $L^2$  is equivalent to the  $l^2$  sequence norm of the wavelet coefficients. According to Parseval's identity (Johnson and Riess (1982)),

$$\|f^t - f^0\|_{L^2}^2 = \|\boldsymbol{\theta}^t - \boldsymbol{\theta}^0\|_{l^2}^2.$$

Thus, the null hypothesis is

$$H_0 : \|\boldsymbol{\theta}^t - \boldsymbol{\theta}^0\|_{l^2}^2 = 0 \text{ for } t = 1, 2, \dots, T$$

indicating that the process is in-control for all times  $t$ . The alternative is that there is some time  $\tau$  after which the functions change:

$$H_a : \|\boldsymbol{\theta}^t - \boldsymbol{\theta}^0\|_{l^2}^2 > 0 \text{ for } t = \tau + 1, \tau + 2, \dots, T.$$

Estimate  $\|\boldsymbol{\theta}^t - \boldsymbol{\theta}^0\|_{l^2}^2$  with  $\|\tilde{\boldsymbol{\theta}}^t - \tilde{\boldsymbol{\theta}}^0\|_{l^2}^2$ . If the in-control profile is known exactly, then so are the DWT coefficients and use  $\tilde{\boldsymbol{\theta}}^0 = \boldsymbol{\theta}^0$ . If the in-control profile must be estimated from a string of assumed in-control observations, then  $\tilde{\boldsymbol{\theta}}^0 \sim \text{normal}(\boldsymbol{\theta}^0, \sigma^2/(mn) \cdot \mathbf{I})$ , where here it is assumed that the in-control profile  $f^0$  was determined by averaging  $m$  in-control profile observations. One may think of the known  $\boldsymbol{\theta}^0$  case as equivalent to setting  $m = \infty$ . Let  $W_t = \frac{n}{\sigma^2} \frac{m}{m+1} \|\tilde{\boldsymbol{\theta}}^t - \tilde{\boldsymbol{\theta}}^0\|_{l^2}^2$ . Then, for each  $t$ ,  $W_t \sim \chi_{n,\gamma}^2$  where

$$\gamma = \frac{n}{\sigma^2} \frac{m}{m+1} \sum_j (\theta_j^t - \theta_j^0)^2 = \frac{n}{\sigma^2} \frac{m}{m+1} \|\boldsymbol{\theta}^t - \boldsymbol{\theta}^0\|_{l^2}^2 \quad (2)$$

is the non-centrality parameter.

Under the null hypothesis that the process is in-control,  $\gamma = 0$ . Under the alternative hypothesis,  $(\tilde{\theta}_i^t - \tilde{\theta}_i^0) \sim \text{Normal}(\theta_i^t - \theta_i^0, \sigma^2(1+1/m)/n)$  due to the orthogonality and linearity of the wavelet transform, implying  $\gamma > 0$  when  $t > \tau$ . Thus, the hypotheses could then be written in terms of  $\gamma$  as:

$$H_0 : \gamma = 0, \quad t = 1, 2, \dots, T$$

$$H_a : \gamma > 0 \quad \text{for } t = \tau + 1, \tau + 2, \dots, T.$$

## 4.2 Likelihood Ratio Test

Assuming  $\sigma$  is known, (this will be relaxed later), the likelihood under the null hypothesis is

$$L_0 = \prod_{t=1}^T f(w_t) = \prod_{t=1}^T \frac{w_t^{n/2-1} e^{-w_t/2}}{2^{n/2} \Gamma(n/2)}.$$

This assumes that the  $W_t$  are independent, which is the case when  $m = \infty$ . For a given  $0 \leq \tau < T$ , the likelihood under the alternative hypothesis is

$$L_a = \prod_{t=1}^{\tau} \frac{w_t^{n/2-1} e^{-w_t/2}}{2^{n/2} \Gamma(n/2)} \prod_{t=\tau+1}^T \left\{ \frac{w_t^{n/2-1} e^{-w_t/2}}{2^{n/2}} \sum_{k=0}^{\infty} \frac{e^{-\gamma/2} (\gamma/4)^k}{k!} \cdot \frac{w_t^k}{\Gamma(n/2 + k)} \right\}.$$

Thus, for any  $0 \leq \tau < T$  the likelihood ratio can be expressed as

$$\frac{L_a}{L_0} = \prod_{t=\tau+1}^T \left\{ \sum_{k=0}^{\infty} \frac{e^{-\gamma/2} (\gamma/4)^k w_t^k}{k!} \cdot \frac{\Gamma(n/2)}{\Gamma(n/2 + k)} \right\}.$$

Using Stirling's approximation (Feller (1968)), this ratio becomes

$$\begin{aligned} \frac{L_a}{L_0} &\approx \prod_{t=\tau+1}^T e^{\gamma(w_t/(2n)-1/2)} \\ &= \exp \left\{ \frac{\gamma}{2n} \sum_{t=\tau+1}^T w_t - \frac{\gamma}{2} (T - \tau) \right\} \\ &= \exp \{ \gamma g(\tau) \}, \end{aligned}$$

where

$$g(\tau) = \frac{1}{2} \sum_{t=\tau+1}^T \left( \frac{w_t}{n} - 1 \right).$$

Thus, for any  $0 \leq \tau < T$  the log of the likelihood ratio is

$$\log \left( \frac{L_a}{L_0} \right) \approx \gamma g(\tau)$$

for fixed  $n$  and  $\sigma$ .

Note that  $E(W_t) = n$  when  $t \leq \tau$ , and  $E(W_t) = n + \gamma$  when  $t > \tau$ , where  $\gamma > 0$  is unknown. These expectations can be estimated as

$$\frac{1}{\tau} \sum_{t=1}^{\tau} w_t \text{ and } \frac{1}{T-\tau} \sum_{t=\tau+1}^T w_t,$$

respectively. A simple estimate of  $\gamma$  is the difference of these two averages. That is,

$$\hat{\gamma} = \frac{1}{T-\tau} \sum_{t=\tau+1}^T w_t - \frac{1}{\tau} \sum_{t=1}^{\tau} w_t. \quad (3)$$

This estimate is preferred over directly estimating  $\gamma$  from (2) since it incorporates information from multiple profiles. One could then write the log likelihood ratio as a function of the unknown  $\tau$  as

$$h(\tau) = \hat{\gamma} \frac{1}{2} \sum_{t=\tau+1}^T \left( \frac{w_t}{n} - 1 \right) \quad (4)$$

and  $\hat{\tau}$  would be the value of  $\tau = 0, 1, \dots, T-1$  that maximizes  $h$ . A drawback of  $\hat{\gamma}$  is its large variance which is on the order of  $n$ . The remaining portion of  $h$  is less variable, having a variance on the order of  $n^{-1}$ . An improved estimator of  $\gamma$  is obtained below by taking advantage of wavelet thresholding.

### 4.3 Thresholding Wavelets to Improve Parameter Estimation

The observed profiles contain noise which must be removed to obtain an accurate estimate of the true underlying profile  $f^t$ . This can be accomplished through the use of wavelet thresholding. If  $\tilde{\theta}_j$  is a wavelet coefficient, then

$$\hat{\theta}_j = \text{sgn}(\tilde{\theta}_j)(|\tilde{\theta}_j| - \lambda)_+$$

is the thresholded coefficient. Using the soft, universal thresholding method (VisuShrink) of Donoho and Johnstone (1994),  $\lambda$  is taken to be  $\sqrt{2\sigma^2 \log(n)/n}$ . This thresholding method

is applied to the difference of the profiles, or equivalently, to the difference of the wavelet coefficients for the two profiles. Let  $\tilde{\theta}_d^t = \tilde{\theta}^t - \tilde{\theta}^0$  and  $\hat{\theta}_d^t$  be the thresholded difference coefficients. The reconstruction of the profile difference using the observed profiles and the thresholded wavelet coefficients is very close to the true difference. In general, the reconstruction error, measured as mean squared error, for the VisuShrink threshold method above is on the order of  $(\log(n)/n)^p$ , where  $p$  is a parameter depending on the smoothness of the functions being considered. This bound implies that the difference of the profiles is being estimated extremely accurately. In particular, the variance of  $\hat{\gamma}$  in (3) is reduced by thresholding.

The new estimate of  $\gamma$  is then the equivalent of (3), with thresholded coefficients replacing the nonthresholded ones. This estimate of  $\gamma$  could be modified through the use of other thresholding methods, such as SureShrink (Donoho and Johnstone (1995)) and the block thresholding methods mentioned earlier. The log likelihood ratio  $h$  in (4) is then a function of the thresholded  $\gamma$  estimate of the function  $g(\tau)$ .

It is now evident that the log likelihood uses wavelets in two fashions. The wavelet coefficients in  $w_t$  measure the size of the difference, while nonlinear thresholded wavelet coefficients are used to determine  $\gamma$  as a function of  $\tau$ .

This can now be implemented as a control chart by maximizing  $h$  over all possible changepoints  $0 \leq \tau < T$  and comparing that maximum value to an upper control limit, UCL. The UCL is found via simulation since the distribution of the test statistic is not known. Thus, having observed  $T > 0$  sample profiles, the proposed method signals that there has been a change in the profiles if

$$h(\hat{\tau}) = \max_{0 \leq \tau < T} h(\tau) > UCL.$$

Once a change in the profiles has been detected,  $\tau$  can then be estimated as

$$\hat{\tau} = \arg \max_{0 \leq \tau < T} h(\tau)$$

and  $\gamma$ , a measure of the magnitude of the change in the profiles, can then be estimated with  $\hat{\gamma}(\hat{\tau})$ .

It can be seen that this method is semiparametric. The likelihood ratio is devised parametrically, but nonparametric methods (nonlinear wavelet thresholding) are used to estimate  $\gamma$ .

The use of thresholding is often associated with monitoring only a select few coefficients. Monitoring only a subset of coefficients leads to the possibility of missing a localized out-of-control condition. This is not the case for the estimator proposed here. All coefficients are examined via the statistic  $W_t$ . Thresholding is used in association with this value by estimating  $\gamma$ .

## 5 Performance of the Changepoint Wavelet Method for Profile Monitoring

The performance of the changepoint wavelet method for monitoring profiles was investigated using Monte Carlo simulation. The piecewise smooth function of Mallat (1999) was used as the in-control profile and several non-linear out-of-control differences between profiles were examined. The in-control function is shown in Figure 1. Although this function is very irregular, it is the difference between profiles that is important. The use of the function in Figure 1 is merely to emphasize that the nature of the profiles is of less importance than the nature of the difference of profiles. This is due to both the estimation abilities of wavelets (they will not smooth over the steep changes like many nonparametric methods) and the differencing step. Additionally, this function was used as the in-control profile in Jeong et al. (2006), so it is included here to improve comparability. Several differences of profiles were examined, as will be discussed below. They range in form from smooth to differences with jumps, and include localized changes, as well.

Standard normal noise was then added to the function in Figure 1. Each sample con-

sisted of a realization of  $n = 512$   $(x, y)$  pairs of such observations. The method was calibrated using a UCL that gives an in-control average run length (ARL) would be approximately 200.

The likelihood ratio devised above assumes that the level of noise  $\sigma$  is known. In practice, this parameter must be estimated. The orthogonality of the DWT provides an easy way in which to accomplish this. The highest level of wavelet coefficients usually models only noise, and any estimator of  $\sigma$  may therefore be applied to this set of coefficients (before any thresholding is performed). In this paper, the median absolute deviation (MAD) is used to estimate  $\sigma$ . Use of MAD rather than other noise estimators such as the sample variance, for example, is standard when estimating noise within a wavelet analysis, since for irregular functions/profiles the highest level of wavelet coefficients might contain profile/function structure (large coefficients). MAD is robust with respect to such outliers. To ensure that the highest level of coefficients truly models noise, only profiles with little or no non-noise characteristics at this level are considered. Each observed profile generates an estimate for  $\sigma$ , so when multiple profiles are observed before an out-of-control condition is signaled, the final estimate of the noise is the average of all the MAD estimates from the observed profiles. The use of the average of the estimates for  $\sigma$  is justified by the weak or strong laws of large numbers.

This estimate of the noise level  $\sigma$  is a within-profile method. An estimate is obtained from each individual profile. The concern of sample size (number of profiles) is diminished if this method is used. If the sampled profile is of length  $n$  then there are  $n/2$  coefficients at the highest detail level of coefficients. So, every observed profile provides  $n/2$  observations with which to estimate  $\sigma$ . The noise level  $\sigma$  is not estimated by examining the between-profile variability. Had this method been chosen, then indeed the number of profiles  $T$  observed becomes an issue. If the first observed profile is out-of-control, then there are certainly not enough observed profiles to form an accurate between-profile estimate of  $\sigma$  by time  $T = 1$ , while the within-profile method used in the proposed estimator has  $n/2$  observations to use.

Note that thresholding does not have an impact on this estimation, since MAD is

applied to pre-thresholded coefficients. In fact, thresholding requires an estimate of  $\sigma$  in its implementation.

The estimation of the UCL depends on whether or not  $\sigma$  is estimated and the value of  $m$ , the number of assumed in-control profiles used to estimate  $f^0$ . To compare the proposed estimator with previous methods, a UCL of 0.029 is used. This corresponds to  $\sigma$  and  $f^0$  both known, a restriction imposed by some of the competing methods.

The UCLs were found via simulation by determining a value such that the ARL for a sequence of flat-line profiles that are always in control is 200. If other values of this ARL are desired, a table of ARL and UCL values are given in Tables 1 through 4. The use of interpolation or regression can provide the appropriate value of a UCL for a desired ARL. Experience has shown that either regressing  $\ln(\text{ARL})$  on UCL, or ARL on  $\text{UCL}^2$  fit the data well. These tables consider multiple values of  $n$  and  $m$ , and whether  $\sigma$  is known or not.

The estimate of  $\gamma$  uses thresholded coefficients, so it might appear that the value of the UCL depends on how many coefficients are available after soft thresholding. However, since the UCL is based on zero-difference profiles, the expected number of these coefficients, say  $n_1$ , is a function only of the sample size  $n$ . Therefore, it is unnecessary to account for the proportion of coefficients not set to zero when determining the UCL. In the simulation results to follow, the ratio  $n_1/n$  is never more than 0.02 for either in-control or out-of-control profile differences.

The performance of the method was first investigated for the situation when there is a simple linear or uniformly additive shift in the profile. That is, a fixed constant  $\sqrt{a} > 0$  was added to the entire in-control profile such the integrated squared error between the in-control profile and the out-of-control profile was  $a$ .

The ARL performance of the changepoint wavelet method for detecting linear shifts in profiles was compared to those of three existing methods. The first alternative method (Fan, 1996) is the uniformly most powerful invariant test using an entire set of wavelet coefficients. This test uses the sum of the squared differences (between the known in-control

profile and a new profile  $f^t$ ) of all the normalized wavelet coefficients. For an in-control profile, the test statistic for this approach is a  $\chi_n^2$  random variable. A discussion of this test and its limitations is given in Fan (1996). We refer to this method as  $M^1$ . The second alternative,  $M^2$ , is the method from Jin and Shi (2001) and is based on examining the subset of the wavelet coefficients determined by applying VisuShrink. Only the non-thresholded coefficients are tested. The third alternative is the method of Jeong et al. (2006), denoted here as  $M^3$ . Their method is similar to Jin and Shi, but uses a different, more data-dependent threshold. For the implementation of the proposed approach, the Haar wavelet is used. All three alternatives were calibrated so that their in-control ARLs were also approximately 200. Some of these competitor methods were designed for use only with known  $f^0$  ( $m = \infty$ ) and  $\sigma$ , rather than their estimates. So, the comparisons in Table 5 incorporate these assumptions in the simulations.

For each estimated ARL, 1000 replications of the study were generated. The results are shown in Table 5. In this table, the proposed nonlinear, semiparametric method is denoted as  $M^*$ . As can be seen for the horizontal line out-of-control condition (i.e., for a simple, uniform additive vertical shift),  $M^*$  has smaller ARL values for detecting out-of-control profiles in all cases but one, and in that case the methods have the same ARL of 1.0, the lowest possible value.

Additionally,  $M^*$  also has the smallest standard deviations for the estimate of the ARL. This is a consequence of applying thresholding in the estimate of  $\gamma$ . The MSE of the estimates  $\hat{\theta}_a^t$  are on the order of  $\ln(n)/n$ , implying that the variance is quite low. With values of  $a$  less than or equal to 0.09, it is evident from the table that the variability for methods  $M^1, M^2$  and  $M^3$  is close to the size of the ARL. This is not true for  $M^*$ .

Besides simple constant or linear differences between profiles, nonlinear out-of-control profile differences were also evaluated. Recall, the only assumption on the difference of the profiles is that they be finite square integrable. Three possible functional forms were investigated for the differences between the in- and out-of-control profiles as shown in Figures

2 (triangular form), 3 (parabolic form), and 4 (broken line). Additionally, another out-of-control profile condition was considered where the out-of-control profile consisted of two localized constant shifts on the intervals between the sample points 89 and 96, and between 241 and 256 (recall there are 512 sample points). This local shift is also considered in Jeong et al. (2006).

Since these are not simple shifts, but somewhat complicated changes, they cannot be easily described in simple terms of vertical displacement as before. Instead, various values are used for  $\|f^0 - f^t\|_{L^2}^2 = a > 0$ , the  $L^2$  norm for the distance between the in- and out-of-control profiles. These shifts represent varying degrees of local to global changes.

The size of  $a$  may also be interpreted in terms of signal-to-noise ratios (snr). The signal-to-noise ratio measures the variability of the function compared to the variability of the errors. Since the method proposed in this paper is detecting the change in profiles rather than estimating profiles directly, the appropriate snr is the variability of the difference function dividing by  $\sigma$ , the variability of the error. For a given  $a$  and  $\sigma$ , these snr are  $a/\sigma^2$  (triangular difference),  $4a/(9\sigma^2)$  (parabolic difference),  $3a/(4\sigma^2)$  (broken line), and  $488a/(512\sigma^2)$  (local shifts difference). The horizontal shift difference function has no variability, so the snr is not defined. In the simulations, values of  $a$  is 0.25 or less, and  $\sigma = 1$ . So the snr's are always 0.25 and smaller.

To compare these results with those  $M^*$  ARL values from the simple horizontal line displacement scenario, the same values were used for  $a$ , the value of the integrated square differences. Again, 1000 replications were performed. Table 5 shows the ARLs for these different forms of the profile differences for  $\tau = 0$ .

It is clear that the proposed  $M^*$  method works best in the simplest case, the horizontal line examined in Table 5. In all cases, however,  $M^*$  works well. For  $a \geq 0.04$ ,  $M^*$  has the lowest ARL and the lowest standard deviations for the ARL.

The proposed  $M^*$  method works best in all but 4 of the 25 total cases examined. In each of those 4 cases,  $M^2$  and  $M^3$  have smaller ARL. It can be noted that when  $M^*$  is better

than  $M^3$ , the ARL of  $M^3$  is regularly 2 to 8 times as large as  $M^*$ . In the 4 cases where  $M^3$  has a lower ARL than  $M^*$ , the ARL for  $M^*$  is never more than 55% higher than the ARL of  $M^3$ . Thus,  $M^*$  is generally more robust than  $M^3$ . A similar observation may be made in the comparison of  $M^2$  with  $M^*$ .

The cases where  $M^*$  performs poorly with regards to the others are all at  $a = 0.01$ . It could be argued that none of the estimators do well at this low level for  $a$ . The standard deviations are just as large as the ARL in all these cases.

Compared with the alternative methods  $M^1$ ,  $M^2$  and  $M^3$ , the  $M^*$  method is unique in that it also provides an estimate of the change point,  $\tau$ , the last sample from the in-control process, as well as an estimate  $\hat{a}$  of the magnitude of the change in the profiles through the use of the thresholded wavelet estimate of  $\gamma$ .

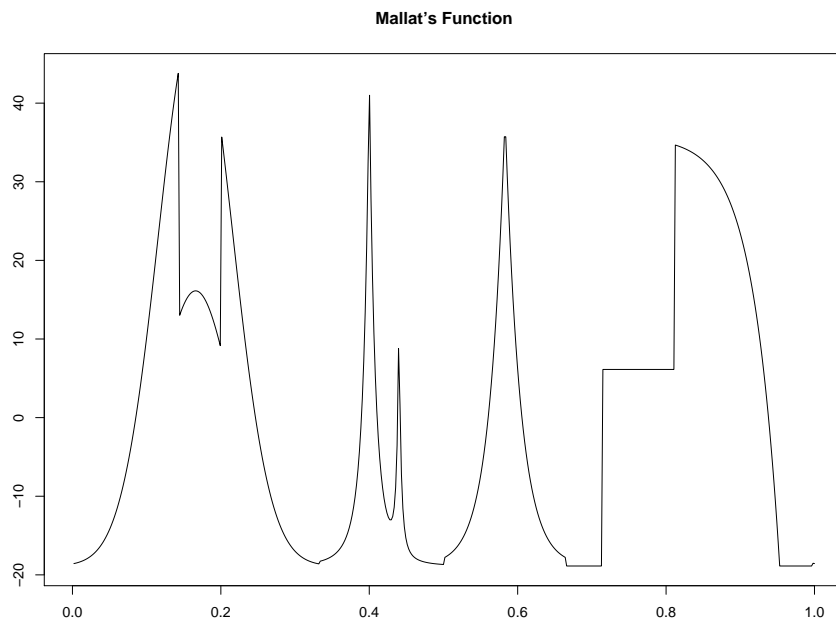


Figure 1: Mallat's piecewise smooth function, Mallat (1999).

Tables 6 through 21 provide a comparison of the ARLs for detecting out-of-control conditions when  $\tau = 0, 10, 25$ , and 50 and the associated estimates of  $\tau$ . The tables also provide  $\hat{a}$ , the wavelet estimate of  $a$ . Comparisons with the competitors is not possible: they

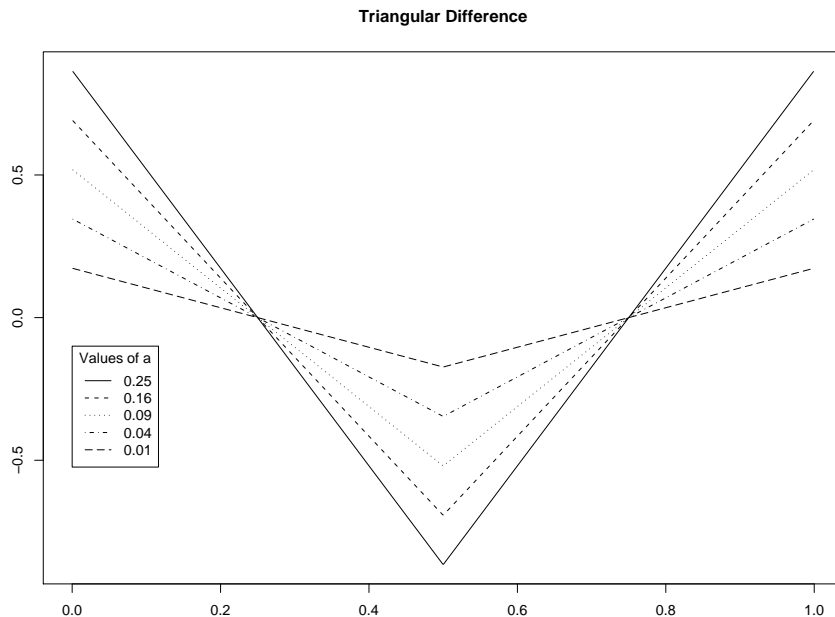


Figure 2: The “Triangular” form for the difference in profiles.

were not designed for such estimates. In these tables,  $\sigma$  is estimated or known, and  $m$  takes on values 5, 10,  $\infty$ .

These tables show several trends. As expected, larger values of  $m$  result in improved estimates and ARLs. Additionally,  $\sigma$  known provides more accuracy in the method than  $\sigma$  estimated. More simulations and UCL values are provided in Chicken et al. (2006).

To illustrate the scale of these values of  $a$  with respect to Mallat’s function, comparisons are shown of this in-control profile and the out-of-control profile in Figures 5 and 6. Here, the out-of-control profile difference is modeled to be of the “Broken Line” form. Figure 5 uses the exaggerated value  $a = 25$  (100 times greater than the largest simulated difference) in order to clearly show the differences between in- and out-of-control profiles. The top panel shows the in-control profile (solid line) with the difference function (dashed line). The center panel shows the in-control (dashed) and out-of-control (solid) profiles, and the bottom panel adds noise to the out-of-control profile. The signal to noise ratio (snr) here is the same as the snr for the simulated cases with  $a = 0.25$  and  $\sigma = 1$ .

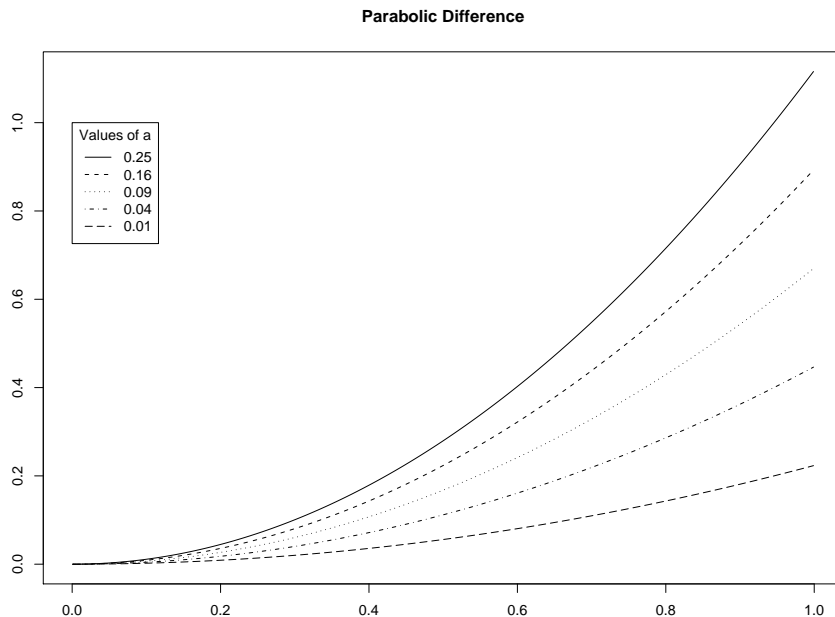


Figure 3: The “Parabolic” form for the difference in profiles.

In the simulation studies, much smaller values of  $a$  were investigated. Figure 6 corresponds to  $a = 0.25$ , the *largest* value of  $a$  that was investigated. Note how the in- and out-of-control profiles in the upper and center panels, respectively, in Figure 6 are nearly indistinguishable from one another. Adding noise to these profiles can only make the difference less apparent visually. Even upon zooming in on the region within the profile where the out-of-control condition resides (Figure 6, bottom panel), it can be seen that for a difference of magnitude  $a = 0.25$ , the change in profiles still appears small. With this in mind, the performance of the  $M^*$  profile change detection method and the changepoint and change magnitude estimators at values of  $a = 0.25$  and less is quite remarkable.

Naturally, the ARL values for  $M^*$  will not be the same when  $\sigma$  and  $f^0$  are unknown. An example is given in Table 22. Here, the estimate of  $\sigma$  is also provided. Three values of  $m$  are used:  $m = \infty$  (corresponding to  $f^0$  being known),  $m = 10$ , and  $m = 5$ . The corresponding UCL values are 0.038, 0.036, and 0.035. Note that decreasing  $m$  increases the ARL values, as expected. The added uncertainty due to fewer in-control candidate profiles

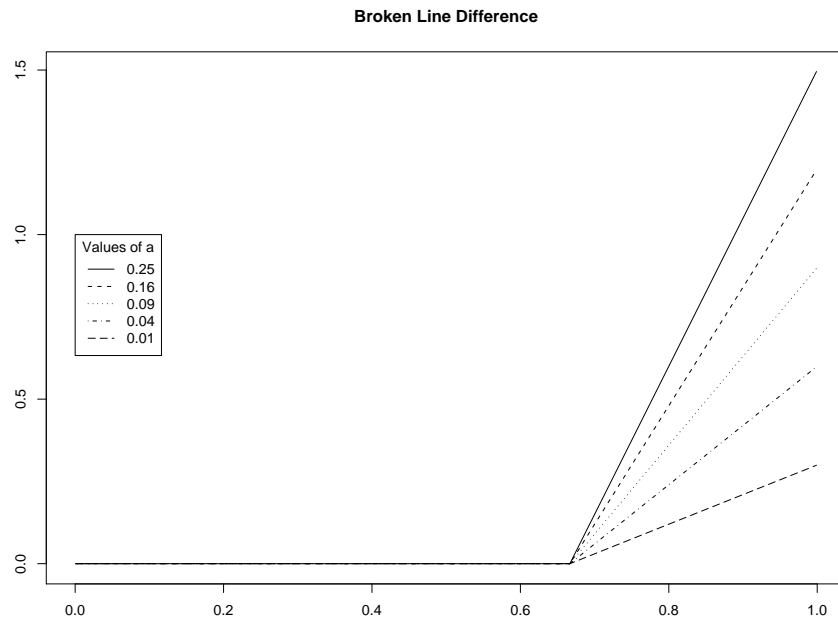


Figure 4: The “Broken Line” form for the difference in profiles.

has little effect on estimates of  $a$ ,  $\tau$  or  $\sigma$ .

The procedure may now be summarized.

1. Obtain an estimate of  $f^0$  by averaging over  $m$  known in-control profiles. If  $f^0$  is known, use  $m = \infty$ . Obtain the DWT of  $f^0$ . Set  $t = 1$ .
2. For observation  $t$ , obtain the DWT of the profile  $f^t$ . Use the highest, most detailed level of wavelet coefficients to estimate the standard deviation of the errors of the observed profile  $f^t$  via the median absolute deviation (MAD). If  $t > 1$ , update the current estimate of  $\sigma$  by averaging over all previous estimates of  $\sigma$ .
3. Threshold the difference of the wavelet coefficients of  $f^0$  and  $f^t$  for use in the estimation of the parameter  $\gamma$  as at (3).
4. Form the likelihood ratio as at (4), and maximize over  $\tau$ .
5. If the result of step 4 is greater than the UCL, signal that an out-of-control profile has been detected and report the value for  $\hat{\tau}$ . Otherwise, go to step 2 and proceed with the new observation at  $t + 1$ .

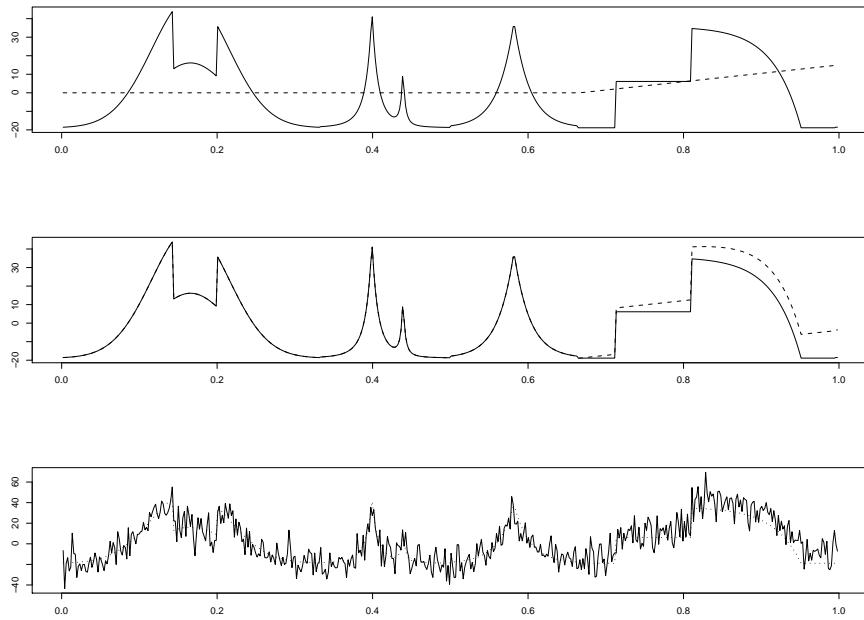


Figure 5: Top panel is the in-control profile (Figure 1), with the “Broken Line” difference (Figure 4) of change magnitude  $a = 25$  added as a dashed line. Center panel is the out-of-control profile (before noise added). Bottom panel adds noise to center panel.

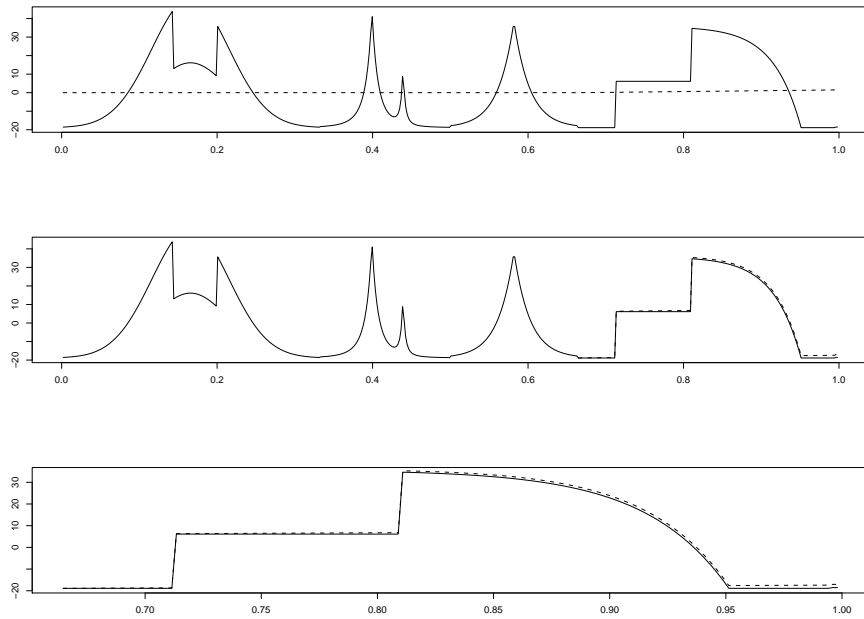


Figure 6: Illustration of out-of-control profile when  $a = .25$ .

$n = 512$		$n = 256$		$n = 128$		$n = 64$	
UCL	ARL	UCL	ARL	UCL	ARL	UCL	ARL
0.015	81.88	0.030	95.78	0.040	64.20	0.100	92.14
0.020	116.06	0.040	137.11	0.060	105.15	0.125	123.24
0.025	164.31	0.050	204.41	0.080	168.66	0.150	161.06
0.030	217.28	0.060	274.40	0.100	237.82	0.175	210.25
0.035	278.39	0.070	344.64	0.120	322.08	0.200	252.00
0.040	353.21	0.080	485.08	0.140	441.77	0.225	308.66
0.045	469.15					0.250	401.09

Table 1: ARLs for various UCLs and values of  $n$ . ( $m = \infty$ ,  $\sigma$  known.)

$n = 512$		$n = 256$		$n = 128$		$n = 64$	
UCL	ARL	UCL	ARL	UCL	ARL	UCL	ARL
0.020	81.59	0.040	89.89	0.080	83.69	0.200	85.00
0.025	106.42	0.050	116.09	0.100	108.74	0.250	117.60
0.030	146.53	0.060	163.42	0.120	137.06	0.300	145.01
0.035	181.65	0.070	193.25	0.140	171.68	0.350	174.57
0.040	218.80	0.080	238.24	0.160	212.91	0.400	213.60
0.045	267.20	0.090	294.49	0.180	259.63	0.450	257.10
0.050	330.45	0.100	350.61	0.200	289.83	0.500	275.16
0.055	388.10	0.110	420.65	0.220	342.92	0.550	334.75
0.060	466.19			0.240	380.66	0.600	363.30
				0.260	402.78	0.650	397.35
						0.700	450.74

Table 2: ARLs for various UCLs and values of  $n$ . ( $m = \infty$ ,  $\sigma$  unknown.)

$n = 512$		$n = 256$		$n = 128$		$n = 64$	
UCL	ARL	UCL	ARL	UCL	ARL	UCL	ARL
0.020	89.77	0.040	88.06	0.080	80.54	0.200	88.96
0.025	121.82	0.050	120.88	0.100	119.04	0.250	121.74
0.030	147.71	0.060	164.43	0.120	152.18	0.300	158.54
0.035	187.42	0.070	203.84	0.140	184.68	0.350	196.48
0.040	214.86	0.080	261.98	0.160	230.99	0.400	225.04
0.045	292.82	0.090	294.19	0.180	284.92	0.450	285.26
0.050	326.40	0.100	367.78	0.200	337.63	0.500	304.31
0.055	403.29	0.110	424.38	0.220	389.33	0.550	382.36
				0.240	465.54	0.600	461.53

Table 3: ARLs for various UCLs and values of  $n$ . ( $m = 10$ ,  $\sigma$  unknown.)

$n = 512$		$n = 256$		$n = 128$		$n = 64$	
UCL	ARL	UCL	ARL	UCL	ARL	UCL	ARL
0.020	93.34	0.040	97.23	0.080	89.48	0.150	69.79
0.025	138.74	0.050	132.82	0.100	127.42	0.200	101.84
0.030	167.08	0.060	185.57	0.120	170.73	0.250	144.90
0.035	202.57	0.070	231.79	0.140	224.80	0.300	185.40
0.040	252.25	0.080	270.21	0.160	293.25	0.350	218.12
0.045	305.60	0.090	345.50	0.180	328.35	0.400	323.26
0.050	372.41	0.100	422.02	0.200	438.26	0.450	354.15
0.055	453.54					0.500	485.19

Table 4: ARLs for various UCLs and values of  $n$ . ( $m = 5$ ,  $\sigma$  unknown.)

Out-of-control profile	$a$				
	0.01	0.04	0.09	0.16	0.25
Horizontal Line					
$M^1$	122.94 (128.82)	34.76 (34.32)	7.97 (7.03)	2.27 (1.69)	1.18 (0.47)
$M^2$	91.36 (94.68)	14.48 (13.47)	2.62 (2.05)	1.14 (0.41)	1.00 (0.04)
$M^3$	71.11 (69.57)	20.76 (19.43)	5.90 (5.01)	2.05 (1.46)	1.17 (0.47)
$M^*$	42.45 (38.36)	2.50 (1.79)	1.14 (0.42)	1.01 (0.09)	1.00 (0.00)
Triangular					
$M^1$	131.50 (129.22)	36.26 (37.11)	8.32 (7.69)	2.28 (1.69)	1.19 (0.47)
$M^2$	90.19 (92.98)	14.33 (13.43)	2.64 (2.08)	1.11 (0.36)	1.01 (0.08)
$M^3$	72.87 (73.10)	21.01 (20.00)	5.88 (5.65)	2.09 (1.51)	1.16 (0.44)
$M^*$	97.94 (84.98)	7.72 (5.94)	1.52 (0.82)	1.03 (0.17)	1.00 (0.03)
Parabolic					
$M^1$	124.55 (123.86)	34.09 (33.72)	7.84 (7.11)	2.23 (1.62)	1.16 (0.44)
$M^2$	84.05 (83.28)	14.57 (13.92)	2.63 (2.05)	1.15 (0.40)	1.00 (0.04)
$M^3$	75.72 (73.49)	21.33 (20.57)	5.63 (5.45)	2.18 (1.61)	1.16 (0.43)
$M^*$	84.62 (72.88)	4.81 (3.80)	1.33 (0.63)	1.03 (0.18)	1.00 (0.00)
Broken Line					
$M^1$	128.24 (130.22)	37.21 (36.05)	7.93 (7.62)	2.27 (1.65)	1.22 (0.50)
$M^2$	91.49 (86.02)	15.52 (14.61)	2.49 (2.07)	1.15 (0.45)	1.00 (0.05)
$M^3$	75.16 (73.82)	20.25 (19.47)	5.52 (4.88)	2.08 (1.48)	1.16 (0.43)
$M^*$	96.96 (81.09)	8.98 (6.96)	1.60 (0.89)	1.05 (0.21)	1.00 (0.03)
Local Jumps					
$M^1$	122.22 (121.19)	35.37 (34.31)	7.70 (7.04)	2.24 (1.66)	1.16 (0.44)
$M^2$	90.17 (92.81)	14.16 (12.91)	2.58 (2.01)	1.12 (0.37)	1.00 (0.04)
$M^3$	72.28 (67.81)	20.72 (21.79)	5.90 (5.20)	2.03 (1.41)	1.16 (0.43)
$M^*$	111.73 (91.68)	11.54 (9.18)	2.09 (1.32)	1.07 (0.26)	1.00 (0.04)

Table 5: ARL comparisons of the four methods,  $\sigma$  known,  $m = \infty$ .

Out-of-control profile	$a$				
	0.01	0.04	0.09	0.16	0.25
Horizontal Line					
ARL	96.22	5.18	2.05	1.29	1.12
$\hat{\tau}$	75.30	3.24	0.76	0.18	0.05
$\hat{a}$	0.04	0.07	0.11	0.18	0.26
$\hat{\sigma}$	0.98	0.98	0.98	0.98	1.00
Triangular					
ARL	128.37	17.97	3.11	1.44	1.13
$\hat{\tau}$	92.35	11.98	1.43	0.30	0.06
$\hat{a}$	0.04	0.05	0.09	0.15	0.22
$\hat{\sigma}$	0.99	0.98	0.98	0.98	0.99
Parabolic					
ARL	132.55	13.09	2.50	1.45	1.12
$\hat{\tau}$	104.03	8.46	1.04	0.33	0.05
$\hat{a}$	0.04	0.06	0.10	0.16	0.24
$\hat{\sigma}$	0.99	0.98	0.98	0.98	0.99
Broken Line					
ARL	123.25	19.83	3.31	1.41	1.16
$\hat{\tau}$	91.14	11.93	1.54	0.28	0.10
$\hat{a}$	0.04	0.05	0.09	0.16	0.25
$\hat{\sigma}$	0.98	0.98	0.97	0.98	0.99
Local Jumps					
ARL	140.25	26.45	4.35	1.68	1.14
$\hat{\tau}$	104.19	14.71	2.08	0.41	0.10
$\hat{a}$	0.04	0.04	0.07	0.13	0.21
$\hat{\sigma}$	0.99	0.98	0.98	0.98	0.99

Table 6: ARLs,  $\hat{\tau}$ ,  $\hat{\sigma}$  and  $\hat{a}$  for various out-of-control profiles with method  $M^*$ ,  $\tau = 0$ ,  $\sigma = 1$ , and  $m = 5$ .

Out-of-control profile	$a$				
	0.01	0.04	0.09	0.16	0.25
Horizontal Line					
ARL	105.73	5.04	1.28	1.04	1.01
$\hat{\tau}$	94.55	11.93	9.19	9.65	9.97
$\hat{a}$	0.04	0.06	0.09	0.16	0.26
$\hat{\sigma}$	0.99	1.00	1.00	1.00	1.00
Triangular					
ARL	138.28	18.95	2.47	1.13	1.00
$\hat{\tau}$	111.32	19.95	10.26	9.78	9.92
$\hat{a}$	0.04	0.05	0.08	0.13	0.21
$\hat{\sigma}$	0.99	1.00	1.00	1.00	1.00
Parabolic					
ARL	132.86	12.52	1.91	1.10	1.01
$\hat{\tau}$	108.86	16.89	9.84	9.76	9.97
$\hat{a}$	0.04	0.05	0.09	0.15	0.24
$\hat{\sigma}$	0.99	0.99	1.00	1.00	1.00
Broken Line					
ARL	147.23	20.90	2.73	1.16	1.01
$\hat{\tau}$	117.23	21.43	10.31	9.74	9.98
$\hat{a}$	0.04	0.05	0.08	0.15	0.24
$\hat{\sigma}$	0.99	0.99	1.00	1.00	1.00
Local Jumps					
ARL	146.46	28.92	3.86	1.31	1.02
$\hat{\tau}$	115.17	24.39	10.80	9.92	9.97
$\hat{a}$	0.04	0.04	0.07	0.12	0.21
$\hat{\sigma}$	0.99	0.99	1.00	1.00	1.00

Table 7: ARLs,  $\hat{\tau}$ ,  $\hat{\sigma}$  and  $\hat{a}$  for various out-of-control profiles with method  $M^*$ ,  $\tau = 10$ ,  $\sigma = 1$ , and  $m = 5$ .

Out-of-control profile	$a$				
	0.01	0.04	0.09	0.16	0.25
Horizontal Line					
ARL	109.21	4.28	1.26	1.03	1.00
$\hat{\tau}$	104.48	25.00	23.71	24.75	24.93
$\hat{a}$	0.04	0.06	0.09	0.17	0.26
$\hat{\sigma}$	1.00	1.00	1.00	1.00	1.00
Triangular					
ARL	152.05	18.79	2.34	1.12	1.00
$\hat{\tau}$	136.87	33.35	24.73	24.70	24.88
$\hat{a}$	0.04	0.04	0.08	0.14	0.21
$\hat{\sigma}$	1.00	1.00	1.00	1.00	1.00
Parabolic					
ARL	142.67	13.72	1.78	1.07	1.01
$\hat{\tau}$	131.15	31.54	24.25	24.68	24.97
$\hat{a}$	0.04	0.05	0.09	0.15	0.24
$\hat{\sigma}$	1.00	1.00	1.00	1.00	1.00
Broken Line					
ARL	153.33	20.81	2.52	1.12	1.01
$\hat{\tau}$	132.38	33.23	24.86	24.65	24.95
$\hat{a}$	0.04	0.05	0.08	0.15	0.24
$\hat{\sigma}$	1.00	1.00	1.00	1.00	1.00
Local Jumps					
ARL	145.53	35.88	3.74	1.28	1.01
$\hat{\tau}$	127.04	40.94	25.31	24.79	24.94
$\hat{a}$	0.04	0.04	0.07	0.12	0.21
$\hat{\sigma}$	0.99	1.00	1.00	1.00	1.00

Table 8: ARLs,  $\hat{\tau}$ ,  $\hat{\sigma}$  and  $\hat{a}$  for various out-of-control profiles with method  $M^*$ ,  $\tau = 25$ ,  $\sigma = 1$ , and  $m = 5$ .

Out-of-control profile	$a$				
	0.01	0.04	0.09	0.16	0.25
Horizontal Line					
ARL	101.43	4.01	1.22	1.03	1.01
$\hat{\tau}$	121.97	48.44	48.30	49.50	49.96
$\hat{a}$	0.04	0.06	0.09	0.16	0.26
$\hat{\sigma}$	1.00	1.00	1.00	1.00	1.00
Triangular					
ARL	156.65	18.20	2.30	1.11	1.01
$\hat{\tau}$	158.54	55.48	49.57	49.53	49.91
$\hat{a}$	0.04	0.05	0.08	0.13	0.22
$\hat{\sigma}$	1.00	1.00	1.00	1.00	1.00
Parabolic					
ARL	140.39	12.38	1.82	1.06	1.00
$\hat{\tau}$	148.19	53.36	48.87	49.69	49.97
$\hat{a}$	0.04	0.05	0.09	0.15	0.24
$\hat{\sigma}$	1.00	1.00	1.00	1.00	1.00
Broken Line					
ARL	152.19	21.37	2.43	1.13	1.01
$\hat{\tau}$	149.16	60.04	49.26	49.68	49.98
$\hat{a}$	0.04	0.05	0.08	0.15	0.24
$\hat{\sigma}$	1.00	1.00	1.00	1.00	1.00
Local Jumps					
ARL	159.95	31.11	3.66	1.28	1.02
$\hat{\tau}$	163.21	60.39	49.87	49.39	49.94
$\hat{a}$	0.04	0.04	0.07	0.12	0.20
$\hat{\sigma}$	1.00	1.00	1.00	1.00	1.00

Table 9: ARLs,  $\hat{\tau}$ ,  $\hat{\sigma}$  and  $\hat{a}$  for various out-of-control profiles with method  $M^*$ ,  $\tau = 50$ ,  $\sigma = 1$ , and  $m = 5$ .

Out-of-control profile	$a$				
	0.01	0.04	0.09	0.16	0.25
Horizontal Line					
ARL	72.06	4.68	1.92	1.28	1.08
$\hat{\tau}$	53.94	2.99	0.69	0.18	0.03
$\hat{a}$	0.04	0.07	0.11	0.18	0.26
$\hat{\sigma}$	0.98	0.97	0.98	0.99	0.99
Triangular					
ARL	115.31	13.20	2.62	1.40	1.06
$\hat{\tau}$	77.62	8.30	1.10	0.27	0.04
$\hat{a}$	0.03	0.05	0.09	0.14	0.22
$\hat{\sigma}$	0.99	0.98	0.98	0.99	0.99
Parabolic					
ARL	103.54	9.24	2.32	1.31	1.08
$\hat{\tau}$	72.11	5.83	0.97	0.19	0.04
$\hat{a}$	0.04	0.06	0.10	0.16	0.25
$\hat{\sigma}$	0.99	0.97	0.98	0.99	0.99
Broken Line					
ARL	113.13	14.67	1.65	1.43	1.11
$\hat{\tau}$	78.69	8.81	1.16	0.28	0.05
$\hat{a}$	0.04	0.05	0.09	0.16	0.25
$\hat{\sigma}$	0.99	0.98	0.98	0.99	1.00
Local Jumps					
ARL	119.22	21.08	3.63	1.55	1.10
$\hat{\tau}$	75.91	12.53	1.68	0.37	0.06
$\hat{a}$	0.04	0.04	0.08	0.13	0.21
$\hat{\sigma}$	0.98	0.98	0.98	0.98	0.99

Table 10: ARLs,  $\hat{\tau}$ ,  $\hat{\sigma}$  and  $\hat{a}$  for various out-of-control profiles with method  $M^*$  and  $\tau = 0$ ,  $\sigma = 1$ ,  $m = 10$ .

Out-of-control profile	$a$				
	0.01	0.04	0.09	0.16	0.25
Horizontal Line					
ARL	75.50	3.51	1.26	1.03	1.00
$\hat{\tau}$	65.66	10.57	9.35	9.74	9.98
$\hat{a}$	0.04	0.06	0.09	0.16	0.26
$\hat{\sigma}$	0.99	1.00	1.00	1.00	1.00
Triangular					
ARL	126.93	13.38	2.03	1.10	1.00
$\hat{\tau}$	94.48	16.71	10.00	9.84	9.98
$\hat{a}$	0.03	0.05	0.08	0.14	0.22
$\hat{\sigma}$	0.99	0.99	1.00	1.00	1.00
Parabolic					
ARL	124.05	8.94	1.63	1.05	1.00
$\hat{\tau}$	97.25	13.68	9.73	9.83	9.98
$\hat{a}$	0.04	0.05	0.09	0.15	0.24
$\hat{\sigma}$	0.99	1.00	1.00	1.00	1.00
Broken Line					
ARL	115.89	14.48	2.22	1.09	1.00
$\hat{\tau}$	86.31	17.13	10.00	9.85	9.97
$\hat{a}$	0.04	0.05	0.08	0.15	0.25
$\hat{\sigma}$	0.99	0.99	1.00	1.00	1.00
Local Jumps					
ARL	126.66	20.82	3.05	1.21	1.01
$\hat{\tau}$	89.01	19.78	10.29	9.92	9.98
$\hat{a}$	0.03	0.04	0.07	0.12	0.21
$\hat{\sigma}$	0.99	1.00	1.00	1.00	1.00

Table 11: ARLs,  $\hat{\tau}$ ,  $\hat{\sigma}$  and  $\hat{a}$  for various out-of-control profiles with method  $M^*$  and  $\tau = 10$ ,  $\sigma = 1$ ,  $m = 10$ .

Out-of-control profile	$a$				
	0.01	0.04	0.09	0.16	0.25
Horizontal Line					
ARL	75.97	3.09	1.17	1.02	1.00
$\hat{\tau}$	80.24	24.12	23.87	24.63	25.00
$\hat{a}$	0.04	0.05	0.09	0.16	0.26
$\hat{\sigma}$	1.00	1.00	1.00	1.00	1.00
Triangular					
ARL	121.30	13.35	1.79	1.06	1.00
$\hat{\tau}$	99.97	30.52	24.40	24.85	24.99
$\hat{a}$	0.03	0.05	0.08	0.14	0.22
$\hat{\sigma}$	1.00	1.00	1.00	1.00	1.00
Parabolic					
ARL	111.18	8.75	1.57	1.03	1.00
$\hat{\tau}$	97.12	28.08	24.12	24.72	24.99
$\hat{a}$	0.04	0.05	0.08	0.16	0.24
$\hat{\sigma}$	1.00	1.00	1.00	1.00	1.00
Broken Line					
ARL	121.93	14.60	2.12	1.08	1.00
$\hat{\tau}$	99.82	30.72	24.71	24.84	24.94
$\hat{a}$	0.03	0.05	0.08	0.15	0.24
$\hat{\sigma}$	0.99	1.00	1.00	1.00	1.00
Local Jumps					
ARL	127.91	20.79	2.89	1.19	1.00
$\hat{\tau}$	105.22	34.33	24.99	24.72	24.99
$\hat{a}$	0.04	0.04	0.07	0.12	0.21
$\hat{\sigma}$	1.00	1.00	1.00	1.00	1.00

Table 12: ARLs,  $\hat{\tau}$ ,  $\hat{\sigma}$  and  $\hat{a}$  for various out-of-control profiles with method  $M^*$  and  $\tau = 25$ ,  $\sigma = 1$ ,  $m = 10$ .

Out-of-control profile	$a$				
	0.01	0.04	0.09	0.16	0.25
Horizontal Line					
ARL	78.55	2.93	1.15	1.02	1.00
$\hat{\tau}$	103.10	48.19	48.55	49.47	49.98
$\hat{a}$	0.04	0.06	0.09	0.17	0.26
$\hat{\sigma}$	1.00	1.00	1.00	1.00	1.00
Triangular					
ARL	130.15	12.71	1.95	1.05	1.00
$\hat{\tau}$	128.49	53.89	48.97	49.73	49.90
$\hat{a}$	0.04	0.05	0.08	0.13	0.22
$\hat{\sigma}$	1.00	1.00	1.00	1.00	1.00
Parabolic					
ARL	110.06	8.06	1.55	1.03	1.00
$\hat{\tau}$	117.98	50.95	48.87	49.56	49.98
$\hat{a}$	0.04	0.05	0.08	0.15	0.25
$\hat{\sigma}$	1.00	1.00	1.00	1.00	1.00
Broken Line					
ARL	133.68	14.63	2.00	1.09	1.00
$\hat{\tau}$	128.40	54.92	49.43	49.66	49.98
$\hat{a}$	0.03	0.05	0.08	0.14	0.24
$\hat{\sigma}$	1.00	1.00	1.00	1.00	1.00
Local Jumps					
ARL	136.18	21.30	2.88	1.15	1.00
$\hat{\tau}$	126.44	56.84	49.63	49.62	49.98
$\hat{a}$	0.03	0.04	0.07	0.12	0.21
$\hat{\sigma}$	1.00	1.00	1.00	1.00	1.00

Table 13: ARLs,  $\hat{\tau}$ ,  $\hat{\sigma}$  and  $\hat{a}$  for various out-of-control profiles with method  $M^*$  and  $\tau = 50$ ,  $\sigma = 1$ ,  $m = 10$ .

Out-of-control profile	$a$				
	0.01	0.04	0.09	0.16	0.25
Horizontal Line					
ARL	48.84	3.93	1.67	1.25	1.08
$\hat{\tau}$	36.66	2.37	0.48	0.15	0.03
$\hat{a}$	0.04	0.06	0.11	0.17	0.26
$\hat{\sigma}$	0.98	0.98	0.98	0.99	0.99
Triangular					
ARL	101.18	9.71	2.14	1.26	1.05
$\hat{\tau}$	64.30	5.72	0.79	0.16	0.03
$\hat{a}$	0.03	0.05	0.09	0.14	0.22
$\hat{\sigma}$	0.98	0.98	0.98	0.99	0.99
Parabolic					
ARL	87.56	7.31	1.99	1.26	1.06
$\hat{\tau}$	58.28	4.41	0.73	0.16	0.02
$\hat{a}$	0.04	0.05	0.10	0.16	0.25
$\hat{\sigma}$	0.98	0.98	0.98	0.99	0.99
Broken Line					
ARL	105.35	10.42	2.37	1.28	1.08
$\hat{\tau}$	67.79	6.14	0.92	0.18	0.04
$\hat{a}$	0.03	0.05	0.10	0.16	0.25
$\hat{\sigma}$	0.98	0.98	0.98	0.99	0.99
Local Jumps					
ARL	108.55	14.35	2.79	1.37	1.07
$\hat{\tau}$	67.18	8.45	1.07	0.23	0.03
$\hat{a}$	0.03	0.04	0.08	0.14	0.22
$\hat{\sigma}$	0.99	0.98	0.98	0.98	0.99

Table 14: ARLs,  $\hat{\tau}$ ,  $\hat{\sigma}$  and  $\hat{a}$  for various out-of-control profiles with method  $M^*$  and  $\tau = 0$ ,  $\sigma = 1$ ,  $m = \infty$ .

Out-of-control profile	$a$				
	0.01	0.04	0.09	0.16	0.25
Horizontal Line					
ARL	57.21	2.73	1.14	1.02	1.01
$\hat{\tau}$	51.67	9.92	9.27	9.88	9.97
$\hat{a}$	0.04	0.05	0.09	0.17	0.26
$\hat{\sigma}$	0.99	1.00	1.00	1.00	1.00
Triangular					
ARL	105.02	9.74	1.68	1.04	1.00
$\hat{\tau}$	78.93	14.74	9.96	9.88	10.00
$\hat{a}$	0.03	0.05	0.08	0.14	0.22
$\hat{\sigma}$	0.99	1.00	1.00	1.00	1.00
Parabolic					
ARL	97.13	6.52	1.44	1.02	1.00
$\hat{\tau}$	69.73	12.68	9.72	9.84	10.00
$\hat{a}$	0.03	0.05	0.09	0.15	0.24
$\hat{\sigma}$	0.99	1.00	1.00	1.00	1.00
Broken Line					
ARL	112.15	10.66	1.86	1.05	1.00
$\hat{\tau}$	78.57	15.25	9.96	9.88	9.99
$\hat{a}$	0.03	0.05	0.08	0.15	0.24
$\hat{\sigma}$	0.99	1.00	1.00	1.00	1.00
Local Jumps					
ARL	115.32	14.77	2.46	1.12	1.00
$\hat{\tau}$	77.73	16.71	10.32	9.93	9.96
$\hat{a}$	0.03	0.04	0.07	0.13	0.22
$\hat{\sigma}$	0.99	0.99	1.00	1.00	1.00

Table 15: ARLs,  $\hat{\tau}$ ,  $\hat{\sigma}$  and  $\hat{a}$  for various out-of-control profiles with method  $M^*$  and  $\tau = 10$ ,  $\sigma = 1$ ,  $m = \infty$ .

Out-of-control profile	$a$				
	0.01	0.04	0.09	0.16	0.25
Horizontal Line					
ARL	52.47	2.59	1.10	1.01	1.00
$\hat{\tau}$	62.79	23.71	23.71	24.81	24.96
$\hat{a}$	0.04	0.05	0.09	0.16	0.26
$\hat{\sigma}$	1.00	1.00	1.00	1.00	1.00
Triangular					
ARL	106.38	25.76	1.62	1.03	1.00
$\hat{\tau}$	88.16	27.80	24.34	24.80	25.00
$\hat{a}$	0.03	0.05	0.08	0.14	0.22
$\hat{\sigma}$	0.99	1.00	1.00	1.00	1.00
Parabolic					
ARL	129.20	6.16	1.39	1.02	1.00
$\hat{\tau}$	84.85	26.40	24.22	24.78	24.99
$\hat{a}$	0.03	0.05	0.09	0.15	0.25
$\hat{\sigma}$	0.99	1.00	1.00	1.00	1.00
Broken Line					
ARL	114.08	10.51	1.68	1.03	1.00
$\hat{\tau}$	93.78	28.70	24.51	24.77	24.98
$\hat{a}$	0.03	0.04	0.08	0.15	0.24
$\hat{\sigma}$	1.00	1.00	1.00	1.00	1.00
Local Jumps					
ARL	123.63	15.42	2.22	1.11	1.00
$\hat{\tau}$	95.57	31.29	24.79	24.93	25.00
$\hat{a}$	0.03	0.04	0.07	0.13	0.22
$\hat{\sigma}$	1.00	1.00	1.00	1.00	1.00

Table 16: ARLs,  $\hat{\tau}$ ,  $\hat{\sigma}$  and  $\hat{a}$  for various out-of-control profiles with method  $M^*$  and  $\tau = 25$ ,  $\sigma = 1$ ,  $m = \infty$ .

Out-of-control profile	$a$				
	0.01	0.04	0.09	0.16	0.25
Horizontal Line					
ARL	53.28	2.42	1.10	1.02	1.00
$\hat{\tau}$	80.90	48.21	48.71	49.77	50.00
$\hat{a}$	0.04	0.05	0.09	0.16	0.26
$\hat{\sigma}$	1.00	1.00	1.00	1.00	1.00
Triangular					
ARL	111.28	8.98	1.59	1.03	1.00
$\hat{\tau}$	107.91	51.51	48.97	49.76	50.00
$\hat{a}$	0.03	0.05	0.08	0.14	0.22
$\hat{\sigma}$	1.00	1.00	1.00	1.00	1.00
Parabolic					
ARL	99.62	5.65	1.34	1.01	1.00
$\hat{\tau}$	105.67	50.04	48.94	49.64	49.99
$\hat{a}$	0.03	0.05	0.09	0.15	0.24
$\hat{\sigma}$	1.00	1.00	1.00	1.00	1.00
Broken Line					
ARL	118.57	9.42	1.69	1.03	1.00
$\hat{\tau}$	111.48	52.34	49.42	49.74	49.99
$\hat{a}$	0.03	0.05	0.08	0.15	0.25
$\hat{\sigma}$	1.00	1.00	1.00	1.00	1.00
Local Jumps					
ARL	118.10	15.05	2.21	1.10	1.00
$\hat{\tau}$	108.53	53.51	49.78	49.89	50.00
$\hat{a}$	0.03	0.04	0.07	0.13	0.22
$\hat{\sigma}$	1.00	1.00	1.00	1.00	1.00

Table 17: ARLs,  $\hat{\tau}$ ,  $\hat{\sigma}$  and  $\hat{a}$  for various out-of-control profiles with method  $M^*$  and  $\tau = 50$ ,  $\sigma = 1$ ,  $m = \infty$ .

Out-of-control profile	$a$				
	0.01	0.04	0.09	0.16	0.25
Horizontal Line					
ARL	44.63	2.45	1.13	1.01	1.00
$\hat{\tau}$	34.65	0.85	0.05	0.00	0.00
$\hat{a}$	0.04	0.06	0.10	0.17	0.26
Triangular					
ARL	101.65	7.49	1.57	1.02	1.00
$\hat{\tau}$	70.91	3.72	0.28	0.01	0.00
$\hat{a}$	0.04	0.05	0.08	0.14	0.22
Parabolic					
ARL	82.06	5.19	1.31	1.03	1.00
$\hat{\tau}$	60.63	2.50	0.15	0.01	0.00
$\hat{a}$	0.04	0.05	0.09	0.16	0.24
Broken Line					
ARL	101.79	8.28	1.64	1.03	1.00
$\hat{\tau}$	68.72	4.47	0.30	0.01	0.00
$\hat{a}$	0.04	0.05	0.09	0.16	0.24
Local Jumps					
ARL	101.78	12.31	2.08	1.10	1.00
$\hat{\tau}$	67.17	6.51	0.52	0.06	0.00
$\hat{a}$	0.04	0.04	0.07	0.13	0.22

Table 18: ARLs,  $\hat{\tau}$ , and  $\hat{a}$  for various out-of-control profiles with method  $M^*$  and  $\tau = 0$ ,  $\sigma$  known,  $m = \infty$ .

Out-of-control profile	$a$				
	0.01	0.04	0.09	0.16	0.25
Horizontal Line					
ARL	47.25	2.17	1.07	1.00	1.00
$\hat{\tau}$	47.02	10.12	9.56	9.85	9.99
$\hat{a}$	0.04	0.06	0.09	0.16	0.26
Triangular					
ARL	95.35	7.07	1.51	1.02	1.00
$\hat{\tau}$	73.42	13.36	10.00	9.93	9.99
$\hat{a}$	0.04	0.05	0.08	0.14	0.22
Parabolic					
ARL	87.08	5.14	1.27	1.01	1.00
$\hat{\tau}$	71.40	12.05	9.90	9.87	9.99
$\hat{a}$	0.04	0.05	0.09	0.15	0.24
Broken Line					
ARL	95.64	8.24	1.57	1.03	1.00
$\hat{\tau}$	75.68	14.10	10.00	9.94	9.99
$\hat{a}$	0.04	0.04	0.08	0.15	0.24
Local Jumps					
ARL	98.08	11.53	2.10	1.06	1.00
$\hat{\tau}$	76.94	15.55	10.39	9.95	10.00
$\hat{a}$	0.04	0.04	0.07	0.12	0.22

Table 19: ARLs,  $\hat{\tau}$ , and  $\hat{a}$  for various out-of-control profiles with method  $M^*$  and  $\tau = 10$ ,  $\sigma$  known,  $m = \infty$ .

Out-of-control profile	$a$				
	0.01	0.04	0.09	0.16	0.25
Horizontal Line					
ARL	45.73	2.09	1.06	1.00	1.00
$\hat{\tau}$	58.49	24.70	24.20	24.86	25.00
$\hat{a}$	0.04	0.05	0.09	0.17	0.26
Triangular					
ARL	96.12	7.51	1.52	1.01	1.00
$\hat{\tau}$	88.72	27.99	24.90	24.81	24.98
$\hat{a}$	0.04	0.05	0.08	0.14	0.22
Parabolic					
ARL	85.71	5.12	1.25	1.01	1.00
$\hat{\tau}$	83.25	26.73	24.72	24.90	24.99
$\hat{a}$	0.04	0.05	0.09	0.15	0.24
Broken Line					
ARL	97.87	8.15	1.56	1.02	1.00
$\hat{\tau}$	89.11	28.71	24.99	24.90	24.99
$\hat{a}$	0.04	0.05	0.08	0.15	0.24
Local Jumps					
ARL	102.08	11.46	2.03	1.07	1.00
$\hat{\tau}$	92.61	30.48	25.21	24.96	24.99
$\hat{a}$	0.04	0.04	0.07	0.13	0.22

Table 20: ARLs,  $\hat{\tau}$ , and  $\hat{a}$  for various out-of-control profiles with method  $M^*$  and  $\tau = 25$ ,  $\sigma$  known,  $m = \infty$ .

## 6 Radar Signature Example

The proposed method was applied to profiles of military radar signatures. For this example, military radar signatures (profiles) of a specific target (such as a vehicle or ground location of interest) were obtained. The exact nature of the specific target cannot be disclosed for security reasons. Changes from a known profile of the target could indicate, for example,

that a vehicle had moved or that some new ground activity was taking place. Profiles were obtained of radar signatures of the same target taken at different times. The radar profiles were aligned to account for transmitter movement between the recording of each profile. The in-control profile was determined from a smoothed average of several profiles from the same target. See Figure 7.

The sequence of profiles was analyzed via the proposed  $M^*$  method. Profile 1 was classified as being in-control. This assessment was confirmed by the radar data source as being correct since there was no change in the target. The  $M^*$  method indicated that profile 2 was different from the known in-control profile and thus was “out-of-control”. Again, the radar data source confirmed that the target had changed after profile 1 and prior to profile 2 so this assessment was correct. Thus, the  $M^*$  method was effective in detecting changes in these radar signature profiles and did so in the shortest possible time, i.e., immediately after the out-of-control condition occurs. Permuting the order of the profile sequence did not affect the accuracy of the method. For example, when running the profiles in the sequence 3, 1, 2,  $M^*$  stopped immediately after analyzing profile 3 (the first observed profile) and noted it as out-of-control (the correct assessment).

## 7 Conclusion

Modern data collections often consist of sequences of long strings of observations. These profiles may be analyzed from an SPC viewpoint to determine when a particular sequence has changed from a previous one. The new profile change detection method described in this paper has been shown to work quickly and accurately on this problem. It analyzes differences that take on a great variety of functional forms, not just linear forms as is the case with linear profiling methods, the most well-studied form of profile analysis. When compared with other wavelet-based profiling methods, the proposed method shows improved abilities through its use of prior information, changepoint analysis, and new use of wavelet estimation.

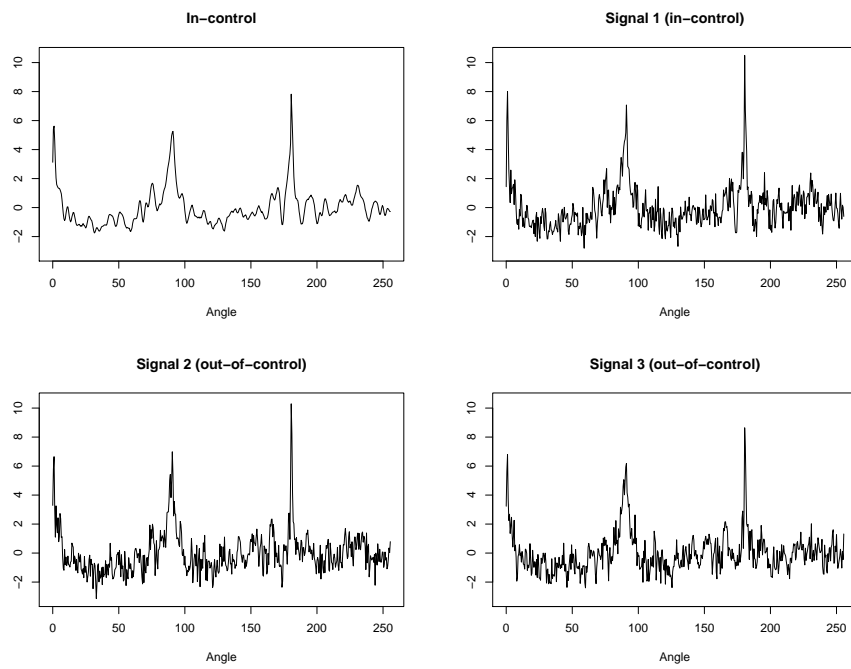


Figure 7: The in-control radar profile and three observed profiles.

Out-of-control profile	$a$				
	0.01	0.04	0.09	0.16	0.25
Horizontal Line					
ARL	47.18	2.16	1.06	1.00	1.00
$\hat{\tau}$	84.53	49.49	49.24	49.85	50.00
$\hat{a}$	0.04	0.05	0.09	0.16	0.26
Triangular					
ARL	93.02	7.45	1.49	1.01	1.00
$\hat{\tau}$	107.18	53.21	49.87	49.91	49.99
$\hat{a}$	0.04	0.05	0.08	0.14	0.22
Parabolic					
ARL	85.50	4.81	1.28	1.01	1.00
$\hat{\tau}$	105.97	51.72	49.62	49.77	49.97
$\hat{a}$	0.04	0.05	0.08	0.15	0.24
Broken Line					
ARL	96.12	8.37	1.54	1.03	1.00
$\hat{\tau}$	115.05	53.66	49.94	49.86	49.99
$\hat{a}$	0.04	0.05	0.08	0.15	0.25
Local Jumps					
ARL	107.57	11.97	1.99	1.08	1.00
$\hat{\tau}$	112.16	54.57	50.28	49.96	49.99
$\hat{a}$	0.03	0.04	0.07	0.12	0.21

Table 21: ARLs,  $\hat{\tau}$ , and  $\hat{a}$  for various out-of-control profiles with method  $M^*$  and  $\tau = 50$ ,  $\sigma$  known,  $m = \infty$ .

	$a$				
	0.01	0.04	0.09	0.16	0.25
$m = \infty$					
ARL	51.84	3.83	1.70	1.20	1.05
$\hat{\tau}$	39.02	2.23	0.51	0.10	0.01
$\hat{a}$	0.04	0.06	0.11	0.18	0.26
$\hat{\sigma}$	0.98	0.98	0.98	0.99	0.99
$m = 10$					
ARL	72.17	4.51	1.80	1.22	1.09
$\hat{\tau}$	54.05	2.72	0.62	0.12	0.04
$\hat{a}$	0.04	0.07	0.11	0.17	0.26
$\hat{\sigma}$	0.99	0.97	0.98	0.98	0.99
$m = 5$					
ARL	84.20	5.51	2.01	1.39	1.12
$\hat{\tau}$	65.58	3.75	0.79	0.25	0.25
$\hat{a}$	0.04	0.07	0.11	0.18	0.26
$\hat{\sigma}$	0.98	0.97	0.98	0.99	0.99

Table 22: ARLs,  $\hat{\tau}$ ,  $\hat{a}$ , and  $\hat{\sigma}$  for horizontal line out-of-control profile with method  $M^*$ ,  $\tau = 0$ , and  $\sigma = 1$ .

## References

- CAI, T. (1999). Adaptive wavelet estimation: A block thresholding and oracle inequality approach. *Ann. Statist.* **27** 898–924.
- CHICKEN, E. (2003). Block thresholding and wavelet estimation for nonequispaced samples. *J. Statist. Plann. Inference* **116** 113–129.
- CHICKEN, E. (2005). Block-dependent thresholding in wavelet regression. *Journal of Non-parametric Statistics* **17** 467–491.
- CHICKEN, E. and CAI, T. (2005). Block thresholding for density estimation: local and global adaptivity. *Journal of Multivariate Analysis* **95** 76–106.
- CHICKEN, E., PIGNATIELLO, J. and SIMPSON, J. (2006). Statistical process monitoring of profiles using wavelets. *Florida State University Department of Statistics Technical Report M976*.
- DAUBECHIES, I. (1992). *Ten Lectures on Wavelets*. SIAM, Philadelphia.
- DING, Y., ZENG, L. and ZHOU, S. (2006). Phase I analysis for monitoring nonlinear profiles in manufacturing processes. *Journal of Quality Technology* **38** 199–216.
- DONOHO, D. and JOHNSTONE, I. (1994). Ideal spatial adaptation via wavelet shrinkage. *Biometrika* **81** 425–455.
- DONOHO, D. and JOHNSTONE, I. (1995). Adapting to unknown smoothness via wavelet shrinkage. *J. Am. Stat. Assoc.* **90** 1200–1224.
- FAN, J. (1996). Test of significance based on wavelet thresholding and Neyman’s truncation. *J. Am. Stat. Assoc.* **91** 674–688.
- FELLER, W. (1968). *An Introduction to Probability Theory and Its Applications, Vol. 1, 3rd ed.* Wiley.

- GARDNER, M., LU, J., GYURCSIK, R., WORTMAN, J., HORNING, B., HEINISCH, H., RYING, E., RAO, S., DAVIS, J. and MOZUMDER, P. (1997). Equipment fault detection using spatial signatures. *IEEE Trans. Compon. Packag. Manuf. Technol. C*, **20** 294–303.
- JEONG, M., LU, J. and WANG, N. (2006). Wavelet-based SPC procedure for complicated functional data. *International Journal of Production Research* **44** 729–744.
- JIN, J. and SHI, J. (1999). Feature-preserving data compression of stamping tonnage information using wavelets. *Technometrics* **41** 327–339.
- JIN, J. and SHI, J. (2001). Automatic feature extraction of waveform signals for in-process diagnostic performance improvement. *J. Intell. Manuf.* **12** 140–145.
- JOHNSON, L. and RIESS, R. (1982). *Numerical Analysis, 2nd ed.* Addison-Wesley.
- KANG, L. and ALBIN, S. (2000). On-line monitoring when the process yields a linear profile. *Journal of Quality Technology* **32** 418–426.
- KIM, K., MAHMOUD, M. and WOODALL, W. (2003). On the monitoring of linear profiles. *Journal of Quality Technology* **35** 317–328.
- MAHMOUD, M., PARKER, P., WOODALL, W. and HAWKINS, D. (2007). A change point method for linear profile data. *Qual. Reliab. Eng. Int.* **23** 247–268.
- MALLAT, S. (1989). Multiresolution approximations and wavelet orthonormal bases of  $L^2(R)$ . *Trans. Amer. Math. Soc.* **315** 69–89.
- MALLAT, S. (1999). *A Wavelet Tour of Signal Processing.* Academic Press.
- MONTGOMERY, D. (2005). *Introduction to Statistical Quality Control.* Wiley.
- OGDEN, R. (1997). *Essential Wavelets for Statistical Applications and Data Analysis.* Birkhauser, Boston.

- STOVER, F. and BRILL, R. (1998). Statistical quality control applied to ion chromatography calibrations. *Journal of Chromatography A* **804** 37–43.
- VIDAKOVIC, B. (1999). *Statistical Modeling by Wavelets*. John Wiley and Sons, New York.
- WILLIAMS, J., WOODALL, W. and BIRCH, J. (2007). Statistical monitoring of nonlinear product and process quality profiles. *Qual. Reliab. Engng. Int.* (in press).
- WOODALL, W., SPITZNER, D., MONTGOMERY, D. and GUPTA, S. (2004). Using control charts to monitor process and product quality profiles. *Journal of Quality Technology* **36** 309–320.
- ZOU, C., ZHANG, Y. and WANG, Z. (2006). A control chart based on a change-point model for monitoring linear profiles. *IIE Transaction* **38** 1093–1103.